IEEE Access
Multidisciplinary ⋮ Rapid Review ⋮ Open Access Journal

Received 24 June 2024, accepted 4 August 2024, date of publication 7 August 2024, date of current version 2 September 2024.

Digital Object Identifier 10.1109/ACCESS.2024.3439889

RESEARCH ARTICLE

Abnormal Gait Classification in Children With Cerebral Palsy Using ConvLSTM Hybrid Model and GAN

YELLE KAVYA[1] AND S. SOFANA REKA[2]
[1]School of Electronics Engineering, Vellore Institute of Technology, Chennai, Tamil Nadu 600127, India
[2]Centre for Smart Grid Technologies, School of Electronics Engineering, Vellore Institute of Technology, Chennai, Tamil Nadu 600127, India

Corresponding author: S. Sofana Reka (sofanareka.s@vit.ac.in)

This work was supported by the Vellore Institute of Technology, Chennai, Tamil Nadu, India.

ABSTRACT Abnormal gait patterns are a common feature of Cerebral Palsy, a neurodevelopmental disease for which early identification is essential for treatment. In the proposed research, a novel methodology is provided for classifying abnormal gait patterns in children with Cerebral Palsy, using gait analysis as a diagnostic tool. To improve gait classification accuracy and efficiency, a hybrid model of Convolutional Long Short-Term Memory (ConvLSTM) model and Generative Adversarial Network (GAN) is used in the suggested technique. The proposed study concentrated on temporal signal data, using hypothetical planes with minimal regard for anatomical indicators. The reduction technique enables a more efficient and successful gait analysis. Heatmap images were created from the selected temporal data. GAN generated images were added to the dataset in order to overcome the problems caused by class imbalance and guarantee a thorough depiction of abnormal gait patterns. In the proposed work, a ConvLSTM-based model with a batch size of 32, training as well as validation datasets were evaluated over a period of 50 epochs. The effectiveness of the suggested model was compared to other models such as Gated Recurrent Unit, Convolutional Neural Network, and Long Short-Term Memory model that were trained using the same input data. Our suggested ConvLSTM model produced an impressive accuracy of 91.8% and a loss of 0.42. The Convolutional Long Short Term Memory model performed better than the other models when compared based on a number of criteria, including accuracy, precision, recall, and F1-score. The performance measures demonstrate how well our method works to classify the abnormal gait in kids with Cerebral Palsy.

INDEX TERMS Cerebral Palsy, convolutional neural network, gait analysis, gated recurrent unit, long short-term memory model.

I. INTRODUCTION

Children with Cerebral Palsy (CP) suffer from a neurological condition that has a significant influence on their motor abilities, coordination, and muscle tone. CP is a complicated and diverse disorder, presenting different difficulties and symptoms for every kid. Children with this disorder face a variety of difficulties that limit their mobility, communication, and day-to-day functioning. Childhood is a period of constant development and discovery. For those with CP, a neurological disorder that profoundly affects development of the child. As a common form of motor disability in childhood, CP affects roughly 1 in 323 children [1]. These numbers highlight how crucial it is for diagnostic efforts to focus on early detection and accuracy. The typical age at which a child with CP is diagnosed is two to three years old [2]. CP has a diverse etiology that can result in this disease. Low birth weight, prenatal infections, oxygen deprivation are the causes that contribute to CP. According to the study stated by Morgan [3], there is a strong correlation between preterm birth and an increased risk of CP. The most prevalent cause of CP is injury to the motor cortex, the area of the brain in charge of controlling voluntary movement. People with CP have motor deficits in their legs when damage occurs

The associate editor coordinating the review of this manuscript and approving it for publication was Liangxiu Han.

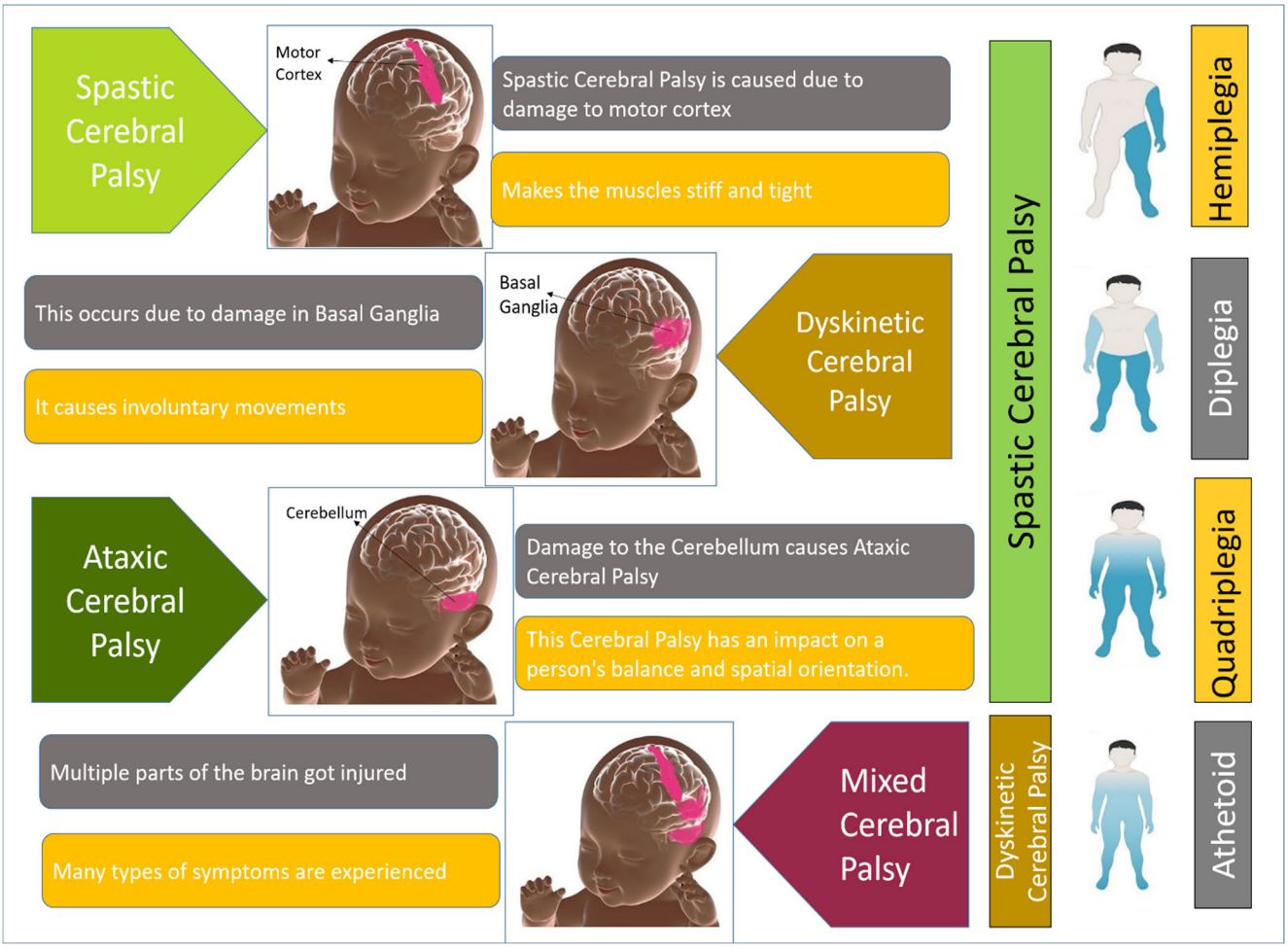

FIGURE 1. Types of Cerebral Palsy and corresponding abnormal gait.

to the area of the motor cortex that controls leg movement. An orthopedic evaluation is essential because hip dislocation, equinus abnormalities, and contractures are caused by muscle imbalance and spasticity [4].

Safety of children with CP while movement is very important. Children with CP benefit greatly from the widespread usage of ankle-foot orthoses as their primary form of gait assistance. Updating these assistive devices should always be prioritized in accordance with user feedback. 'Comfort while wearing' the assistive device is the most crucial feature acknowledged by both specialists and customers [5] which involves preventing skin pressure, friction, or abrasions. There may be a possibility of Intellectual Disability in children with CP [6]. Figure 1 illustrates different parts of the brain affected and their impact on gait and movement.

The muscles of children with spastic CP will be tight and stiff. This spastic CP affects 70% of patients with CP. There are three categories in spastic CP, as depicted in figure 1. One arm and one leg are affected in spastic hemiplegia. In spastic diplegia, both lower limbs are more affected than upper limbs. All four limbs are affected in spastic quadriplegia. Among three types of spastic CP, spastic quadriplegia is the most severe, requiring the patient to rely on assistive devices for support. Athetoid CP, also referred to as dyskinetic CP, is a less common form that affects only ten to twenty percent of CP patients. There will be jerky movements during the gait cycle as a result of this CP. In mixed CP, combinations of gait deformities from spastic, dyskinetic and ataxic are seen.

Despite the fact that CP is not a progressive disorder, indicates that adults with CP has higher chance of developing chronic illnesses. CP has significant societal and economic costs in addition to personal ones. A person with CP may require lifetime care that exceeds $1.5 million to include medical costs, assistive technology, and educational support. These figures highlight the social and economic factors that necessitate all-encompassing methods of providing care and integrating them into society. By the time children with CP reached adulthood, the majority of CP patients had fall often and had decrease in the level of their mobility [7]. Early intervention can improve the child's quality of life and lessen the condition's long-term effects by identifying these gait

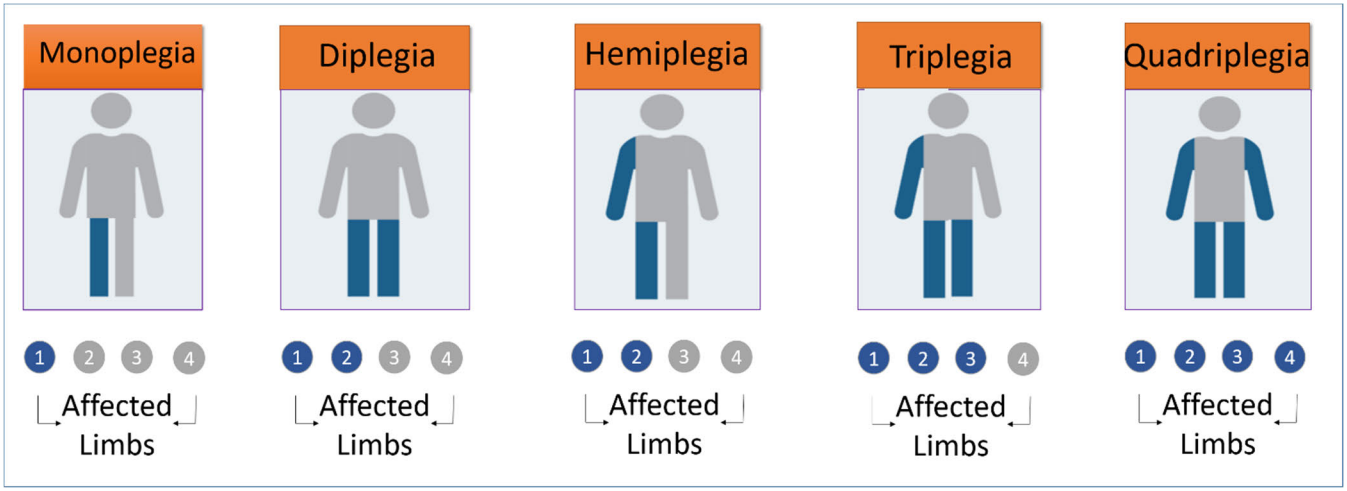

FIGURE 2. Classification of Cerebral Palsy based on affected limbs.

abnormalities. Gait is important in identifying CP during early stages of development.

The prevalence of CP linked to birth problems has dramatically decreased as a result of improvements in medical treatment and interventions. Understanding the complex mechanisms of the brain is essential to recognize the ways in which injury to one region of the brain can impact limbs and other bodily functions. Different limbs of the body gets affected based on the damage to the part of the brain, as depicted in figure 2. In CP, monoplegia refers to the paralysis or severe weakening in one arm or leg. Paralysis or weakness, usually more noticeable in the lower extremities than the upper extremities, is a characteristic of diplegia. Domagalska-Szopa and Szopa [8] demonstrated that lower limb kinematic abnormalities in the sagittal plane were not the only cause of gait abnormalities in children with bilateral CP. Hemiplegia refers to paralysis or weakness affecting the arm and leg on the affected side of the body. Piitulainen et al. [9] stated that gait stability in kids with hemiplegia and diplegia is more complicated than gait in Typically Developed (TD) children and that gait stability may be assessed with the help of the IMU-RCME, or Inertial Measurement Unit-Refined Compound-Multiscale Entropy.

In comparison to hemiplegic patients, the effects were more noticeable in diplegic patients. In CP, triplegia refers to the paralysis or weakening of three limbs, either one arm and one leg or both legs and one arm. When a person has quadriplegic, meaning they are paralyzed or weak in both arms and legs. In the preceding figure 2, affected limbs are highlighted in blue and unaffected limbs are in grey color. Individual's gait patterns can be characterized by spatiotemporal factors, which enables evaluation of their health condition and identification of clinically significant alterations in their gait. Asif et al. [10] used the concepts of static and dynamic equilibrium to examine the spatiotemporal parameters of gait. The examination concentrated on how the knee angles and positions changed as the subject moved, especially in dynamic states, and it showed that these changes were constant and related to changes in the body's condition and speed. Researchers have predicted leg flexion or extension during various activities by utilising positional data and angular movement. Even though it can be difficult to define speed and body state from positional and knee joint angle data, spatiotemporal parameter analysis of this research allows for precise predictions of walking speeds and body states. Carcreff et al. [11] stated that, while collecting the gait data for any classification algorithm, group of children with CP walked fast in the lab than they did when they were walking naturally and the author of the research made a comparison between every parameter recorded in the lab and every parameter measured while walking on a daily basis. The majority of gait traits varied between the two settings.

Kanko et al. [12] measured and compared nine spatiotemporal gait metrics. Mean differences, Pearson correlation coefficients, intra class correlation coefficients, and Bland-Altman methods were used to compare the measurements. These results suggest that spatiotemporal gait parameters can be accurately measured over ground and treadmill locomotion using marker less motion capture. Hussein et al. [13] results indicates that proprioceptive training combined with visual feedback during gait training is more successful than traditional gait training for improving the spatial and temporal gait features of children with diplegic CP. Steffensen et al. [14] concurrently gathered both marker-based and markerless data. Time-series waveforms of 3D ankle, knee, hip, and trunk angles were stride adjusted and compared when assessing gait kinematics in individuals with CP. This demonstrates how Theia3D tracking for markerless motion capture produces results that are in good agreement with marker-based techniques. Lorentzen et al. [15] proposed that children with CP may have better gait during push off in late stance, which can be improved with rigorous treadmill

training. Exercise promotes the central drive to the ankle plantar flexors and lessens asymmetry in gait. In addition to offering a quantitative and objective evaluation of gait impairments, gait analysis is helpful in assessing the effectiveness of treatment. Gait analysis can improve, broaden, and maximize patients' therapy regimens [16]. Ma et al. [17] proposed Kinect is a useful clinical gait analysis tool for kids with CP because it is potential for the gait analysis system to enhance its lower limb kinematics measurement capabilities. The findings indicate that sagittal angles at the hip and knee were more precise, and the LSTM method had the benefit of increasing the accuracy of the ankle tracking. Oudenhoven et al. [18] adopted multilevel analysis to evaluate the effects of training at different walking velocities. Children's self-selected comfortable walking speed increased to 0.85 ± 0.25 m/s from 0.71 ± 0.25 m/s.

One of the main characteristics of CP is spasticity, which is characterized by rigidity and elevated muscular tone. Walking-related issues include hyperactive and stretch-resistant muscles that makes difficult to initiate and control movements. In CP, prolonged stiffness and muscular imbalance can result in joint contractures. Wesseling et al. [19] proposed EMG-restricted optimization, the EMG (Electromyography) of eight muscles was employed as the muscular excitation signal, limiting the muscle activation patterns and enabling the determination of muscle forces.

Metabolic power in children with CP is usually two times higher than in their contemporaries with typical development. Gill et al. [20] employed Bayesian additive regression trees to evaluate the causal consequences of CP gait and the findings imply that interventions aimed at enhancing gait pattern may be more advantageous. Based on the walking pattern, gait in CP are classified into four types, jump gait, true equinus, apparent equinus and crouch gait as illustrated in figure 3.

A fixed downward-pointing or plantarflexed ankle joint is often the result of calf muscular spasticity which is used to classify true equinus. Persistent toe walking brought on by an inadequate dorsiflexion of the foot in plantarflexed ankle joint type of gait. Children with equinus gait demonstrated improved gait following repeated therapy with Botulinum Toxin type A (BTX-A) injections, according to author's study [21]. The greater bending of the knee and ankle during the swing phase is the primary characteristic that distinguishes jump gait from other gaits. In this gait, a discernible upward motion, almost like a leap, particularly in the swing stage can be seen. The appearance of particular foot positions, such as equinus, that may look fixed throughout walking, is used to classify apparent gait. In this gait, compensatory motions can be noticed in other joints, which provide the impression of immobile foot postures. Excessive bending at the hips, knees, and ankles during walking is the basis for classifying crouch gait. Pronounced hunching over or squatting while moving can be seen in this gait. In order to extract the features from the croach gait, Shideler et al. [22] developed a graphical user interface to digitally alter the stimulation parameters, timing, and intensity during walking and author suggested precise application of electrical stimulation to the quadriceps is a potential treatment for the crouch gait. Ries et al. [23] proposed that both ground reaction ankle-foot orthosis (GRAFO) and the solid ankle-foot orthosis (SAFO) designs are equally effective at correcting crouch gait and at reversing it in individuals with CP. Snodgrass et al. [24] created a wearable, cable-driven robotic system that gives children with CP controlled disruption to their knee joints as they walk over ground which improves the gait in better way. Liu et al. [25] suggested a technique known as Deep Rehabilitation Gait Learning (DRGL) which makes use of LSTM to demonstrate the gait feature's inherent spatial-temporal associations. Instead of requiring intricate kinematic and dynamic models for the human body and exoskeleton, DRGL allows unusual knee joint trajectories to be anticipated and rectified based on the wearer's other joints.

The aim of proposed work is to significantly advance the field of pediatric neurology by classifying abnormal gait in children with CP. For the classification of abnormal gait in CP, a novel Convolutional Long Short Term Memory (ConvLSTM) model is presented by using gait data of children with CP and advanced DL techniques which enhances the quality of life for kids with early detection and classification. Firstly, the time series gait signal data is converted to images and produced a rich set of heatmap images. Interestingly, we build upon this breakthrough by using Generative Adversarial Network (GANs) to produce more images in order to overcome class imbalance problem. The original data along with GAN generated data is utilized in a Convolutional Long Short-Term Memory (ConvLSTM) model to improve the categorization of children with CP based on their gait patterns. The innovative approach not only builds on previous developments but also pioneers the merging of GANs and ConvLSTM in the field of gait analysis. The proposed study aims to maximize the gait analysis procedure through a deliberate reduction in the quantity of anatomical markers used (where the markers are placed on ankle, hip, and knee, avoiding markers on the trunk and pelvis).

The manuscript is organized as follows: section I speaks about introduction. Section II offers a thorough review of the literature, highlighting recent findings and developments that are relevant to the research topic. Section III consists of three sub sections which illustrates dataset details, preprocessing steps and proposed methodology. The results and performance metrics of the proposed ConvLSTM model are presented in Section IV. Section V offers an overview of the major findings and conclusions derived from the research. Finally, section VI speaks about Limitations and Future Scope.

II. LITERATURE SURVEY

Recent advances in technology, notably the incorporation of Machine Learning (ML) and Deep Learning (DL) techniques, have brought about significant changes in the field of gait analysis. The popularity of ML as well as DL approaches in the gait domain is because they can quickly, reliably,

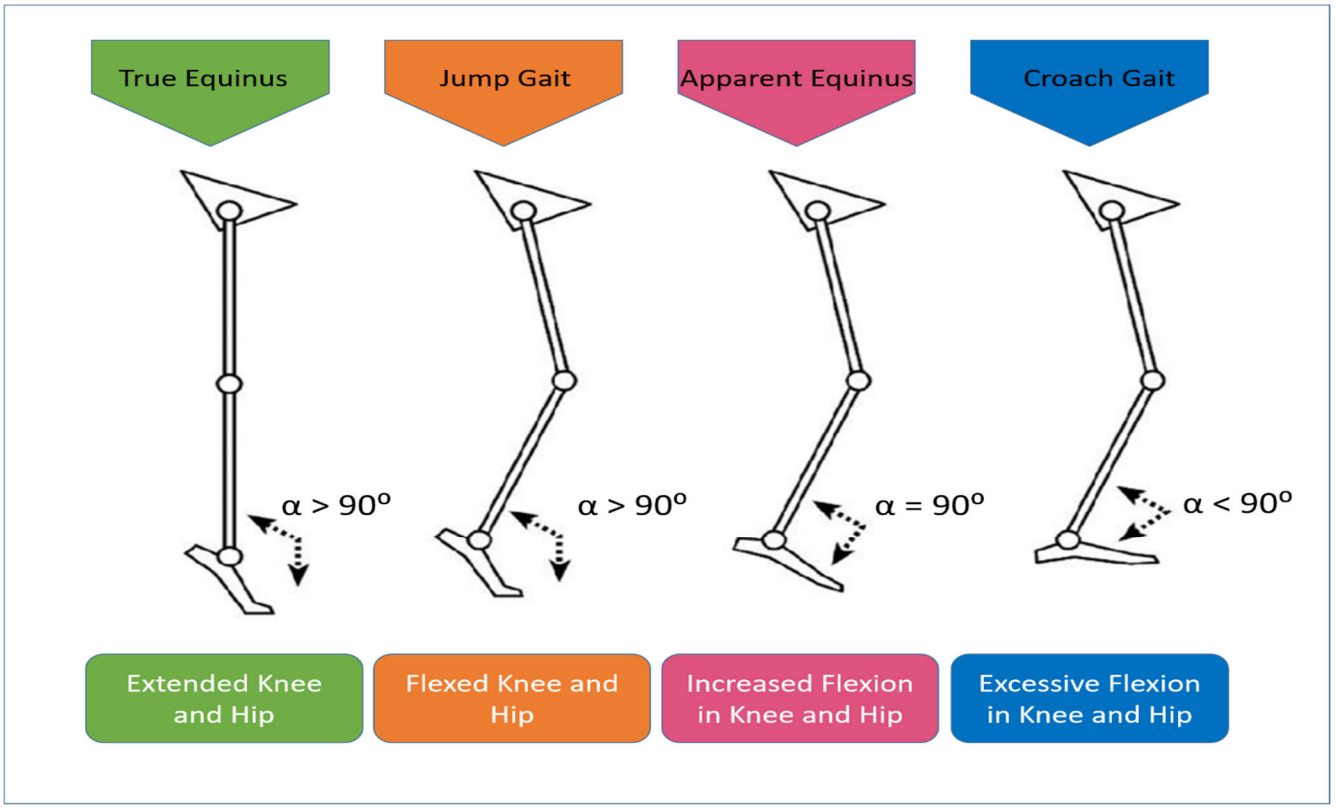

FIGURE 3. Gait patterns in Cerebral Palsy.

and accurately classify data by extracting basic features from highly temporal and nonlinear biomechanical data [26]. Kolaghassi et al. [27] proposed four deep learning models which are trained on typically developed children's gait where he suggested that Fully Connected Network (FCN) and Transformer algorithms performed well because of their low errors. Joint moments of CP patients were estimated by the author [28] with normalized Root Mean Square Error (nRMSE) ranging from 18.02% to 13.58% by training specific CNN model. Based on the meta analysis done by the author [29], CNN achieved exceptional results in the diagnosing CP and multiple sclerosis. Lempereur et al. [30] introduced a long short term memory recurrent neural network with the special application DeepEvent. The automatic detection of gait events was implemented using three bidirectional LSTM layers, each with eight hundred hidden units. These discoveries have greatly expanded understanding of gait patterns and created new opportunities for the creation of more effective treatments for conditions like CP. Al-Sowi et al. [31] assessed the children with CP using five well-known machine learning classification techniques. The MLP classifier properly classified CP-type cases with an accuracy rate of 84%. Zhang and Ma [32] classified the gait of children with CP who had spastic diplegia where the classification of gait was done based on the kinematic features of their lower limbs. The performance of the algorithms was assessed using a conventional 10-fold cross-validation technique. According to the results, the ANN has the lowest resubstitution error (5.8%) and the best prediction accuracy (93.5%). Patil et al. [33] examined and evaluated the performance of four machine learning techniques (KNN, SVM, ELM, and MLP) for multi-class gait classification. Out of four techniques, ELM performed well in classification of gait patterns. The author employed a data-driven methodology [34] to estimate the frequency of foot-off and foot-contact events in children with normal and pathological gait based on kinematic and marker time series. More precise real-time forecasts of foot-off and foot-contact events are made possible by the LSTM architecture. Potluri et al. [35] presented a wearable sensor system that combines inertial measurement units (IMUs) and plantar pressure measurement units which is combined with stacked LSTM for identifying gait defects. The simulated pathological and normal gaits showed a marked difference in gait characteristics, which was detected by the proposed stacked LSTM recurrent neural network. McCay et al. [36] extracted the normalized pose-based feature data, Joint Orientation 2D Histograms and Joint Displacement 2D Histograms, for use in new deep learning architectures. Experimental results showed that the proposed fully connected neural network (FCNet) functioned wonderfully across a range of feature sets.

The application of CNN and LSTM networks in the context of gait analysis has been studied in the literature survey [28], [29], [30], [34], [35]. Previous research has demonstrated impressive progress in employing sophisticated neural network architectures and training them with diverse forms of gait data, such as kinematic, kinetic, and spatiotemporal data, where this study takes a novel approach to classify abnormal gaits in children with CP. CNNs have proven to be efficient at extracting spatial characteristics from gait data in the literature, and LSTMs have proven to be expert at managing sequential dependencies in temporal data. The proposed research expands on earlier research by putting forth a novel hybrid model that combines the best features of both CNNs and LSTMs for identifying abnormal gaits in kids with CP, we hope to fill a large vacuum in the literature. Through the transformation of temporal data into heatmap images and the utilization of GAN-generated images in conjunction with the original data, classification system's resilience and interpretability are improved. Our objective is to create and evaluate a hybrid CNN-LSTM model that can effectively categorize children with CP according to their abnormal gaits, while simultaneously addressing the issue of class imbalance by utilizing GAN-generated data in a strategic manner. This specific goal directs our approach and offers a strong basis for expanding the body of knowledge in the field of gait analysis and enhancing the clinical results for children with CP.

III. MATERIALS AND METHODS

Figure 4 displays the overview of our approach. The time series data of angles formed by movements of the hip, ankle, and knee with respect to the sagittal and coronal planes are examined in the CSV dataset. Preprocessing steps of cleaning, normalizing, and segmenting the time series data are done in the process. Time series features for the hip, ankle, and knee are taken from this data and transformed into images. Each time series feature is displayed as a heatmap image in this step, which involves a transition from the time domain to the spatial domain. The procedure is creating heatmap images with Python, which offer a clear depiction of temporal trends. The following stage involves producing more images using GAN. The original time series image's distribution is learned by the GAN, which then creates new images that depict similar patterns. For the classification problem, ConvLSTM model is put forward. ConvLSTM is a neural network architecture designed for processing spatiotemporal data, including image sequences. Using both the original and GAN-generated images as input, the ConvLSTM model learns to categorize gait data into abnormal gait A, B, C, and D categories. Using the labeled dataset, where each image is linked to a certain gait type, model is trained and tested in 80:20 ratio. The 20% of converted images are manually selected which belongs to seven extracted features from the dataset, strictly excluding GAN generated images. For an accurate assessment of the model's performance on actual data, segregating test set with original images alone was essential. Training was conducted using the remaining 80% of the dataset consists of both original and GAN-generated images to improve the model's robustness and learning capabilities. In the sections that follow, each and every step of this suggested work flow is covered in detail.

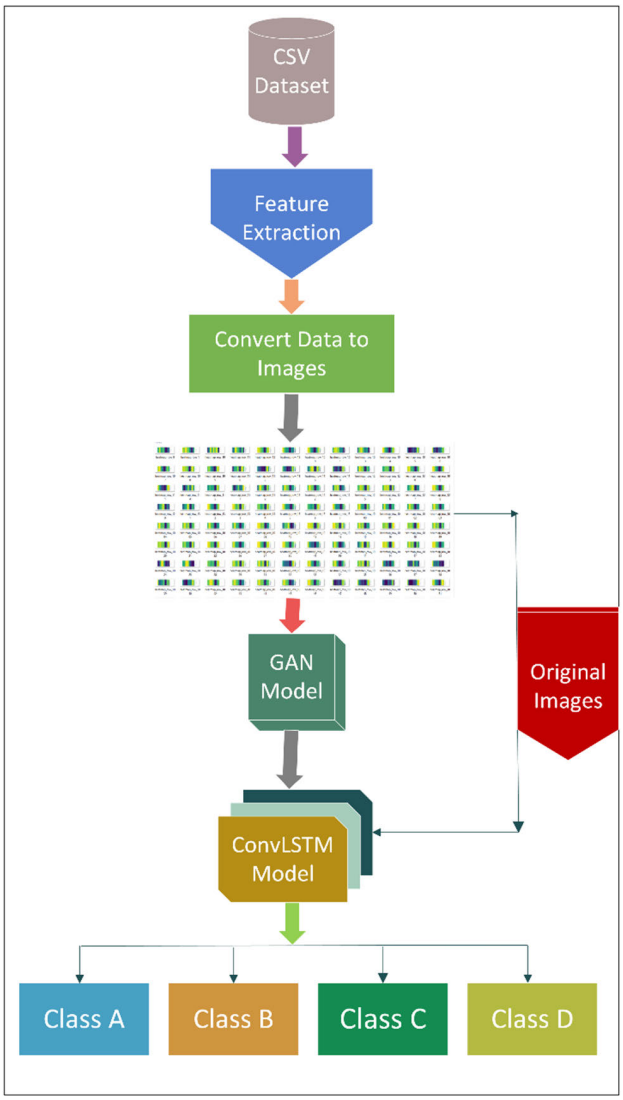

FIGURE 4. Proposed work flow.

A. DATASET DESCRIPTION

Initial data exploration gives valuable insights into data distribution and forms the basis for subsequent analysis. The rich dataset is used in the proposed work which is present in publicly accessible CSV file [37] includes 744 feature parameters and 1719 samples from 357 participants. This publicly available data was collected from gait analysis sessions involving children aged three to eighteen who had unilateral or bilateral spastic CP at University Hospital Pellenberg's clinical motion analysis lab. Youngsters exhibiting symptoms of dystonia or ataxia are eliminated from the mentioned dataset.

TABLE 1. Extracted features from the dataset.

Feature	Description
aSagH	Angle made by hip with respect to sagittal plane
avSagH	Average angle made by hip with respect to sagittal plane
aCorH	Angle made by hip with respect to coronal plane
aSagK	Angle made by knee with respect to sagittal plane
avSagK	Average angle made by knee with respect to sagittal plane
aSagA	Angle made by ankle with respect to sagittal plane
avSagA	Average angle made by ankle with respect to sagittal plane

Vicon Motion Systems was used to conduct a standardized 3DGA (3D Gait Analysis) examination and gather the data. Clinical professionals applied reflective markers in line with the Plug-In-Gait marker configuration to the child's lower leg anatomical landmarks. Using the Nexus software, the joint angles and their derivatives were determined.

Feature parameters of hip, ankle and knee with respect to multiple planes like sagittal and coronal are selected for the data analysis. Table 1 displays the selected features details.

The time-series data of joint angles measured at various instances of gait cycle are included in the dataset. The data spans from the 0th instance, which indicates the start of the gait cycle, to the 1000th instance, which is end of the cycle representing 100% of the cycle. For the proposed work, time series feature data 'aSagH_pct_GC' is considered from 'aSagH_pct_GC_0' to 'aSagH_pct_GC_1000'. Similarly, time series data of remaining six features avSagH_pct_GC, aCorH_pct_GC, aSagK_pct_GC, avSagK_pct_GC, aSagA_pct_GC, avSagA_pct_GC also included in the analysis. Total 350 columns time series data of seven features with 1719 samples from the dataset [37] are considered for the proposed work. Table 1 lists the seven extracted features, which include the angles and average joint angles of the hip, ankle, and knee with respect to the sagittal and coronal planes. Angles at every instance of the gait cycle is measured for these features. Joint angles measured at various points during the gait cycle are used to categorize gait patterns in people with CP. These measurements are essential for distinguishing abnormalities and comprehending the various phases of the gait in CP. The graphs of three different CP gait pattern samples are displayed in Figure 5, which illustrates the analysis on distinct gait phases in abnormal gaits.

B. DATA PREPROCESSING

In the preprocessing pipeline, firstly all relevant feature columns are manually selected. The data is imported from a CSV file, and the scikit-learn library's LabelEncoder was used to convert category columns into numerical labels. This stage made it easier to convert categorical data that isn't quantitative into a format that can be analysed. To avoid ordinality assumptions, one-hot encoding was then used to further process the category characteristics by turning them into binary vectors. Zeros were used to impute any missing values in order to preserve the integrity of the data. After that, every piece of data was converted into a numeric format to maintain consistency throughout the dataset. After a part of preprocessing is completed, signal time series data at discrete time instances of gait cycle $t_0, t_1, t_2 \ldots t_n$ for one sample is represented in (1).

$$Smn = \{Sm_0, Sm_1, Sm_2, \ldots .Smn\} \tag{1}$$

Here 'm' represents number of samples present in the dataset and 'n' represents the number of time instances of gait cycle. 'S_{mn}' represents signal value at 't'_n for '$m^{th'}$ sample in the dataset.

From the dataset, all 1719 samples are considered for a feature and represented in matrix format displayed in (2)

$$X = \begin{bmatrix} S_{00} & S_{01} & \cdots & S_{0n} \\ S_{10} & S_{11} & \ldots & S_{1n} \\ \vdots & \vdots & \ddots & \vdots \\ S_{m0} & S_{m1} & \cdots & S_{mn} \end{bmatrix} \tag{2}$$

Here 'S_{mn}' represents signal value at 'm^{th}' sample for 'n^{th}' time instant.

Min-Max scaling was performed on 'X' to rescale all numerical attributes to a range between 0 and 1, reducing the impact of different scales and ranges among features.

$$S'_{\mathrm{mn}} = \frac{\mathrm{S_{mn}} - \mathrm{Min\ (X)}}{\mathrm{Max\ (X)} - Min\ (X)} \tag{3}$$

In (3), *Max (X)* and *Min (X)* are represented as maximum and minimum values of the matrix X.

Regardless of the feature's initial scale, normalization process made sure that each data contributed proportionately to the analysis by normalizing the signal values to the range [0, 1] using Min Max scaling.

The preprocessed data will now be converted into heatmap images. Heatmap images were created from signal data which is already encoded using one hot and label encoding and normalized using Min-Max scaling. The data representation was improved by this change, giving complete information of the training participants. Once thorough preprocessing is completed, will go through data conversion process. The code extracts the data corresponding to the chosen feature columns by looping through each row of the preprocessed data frame. From the retrieved data, a heatmap is created

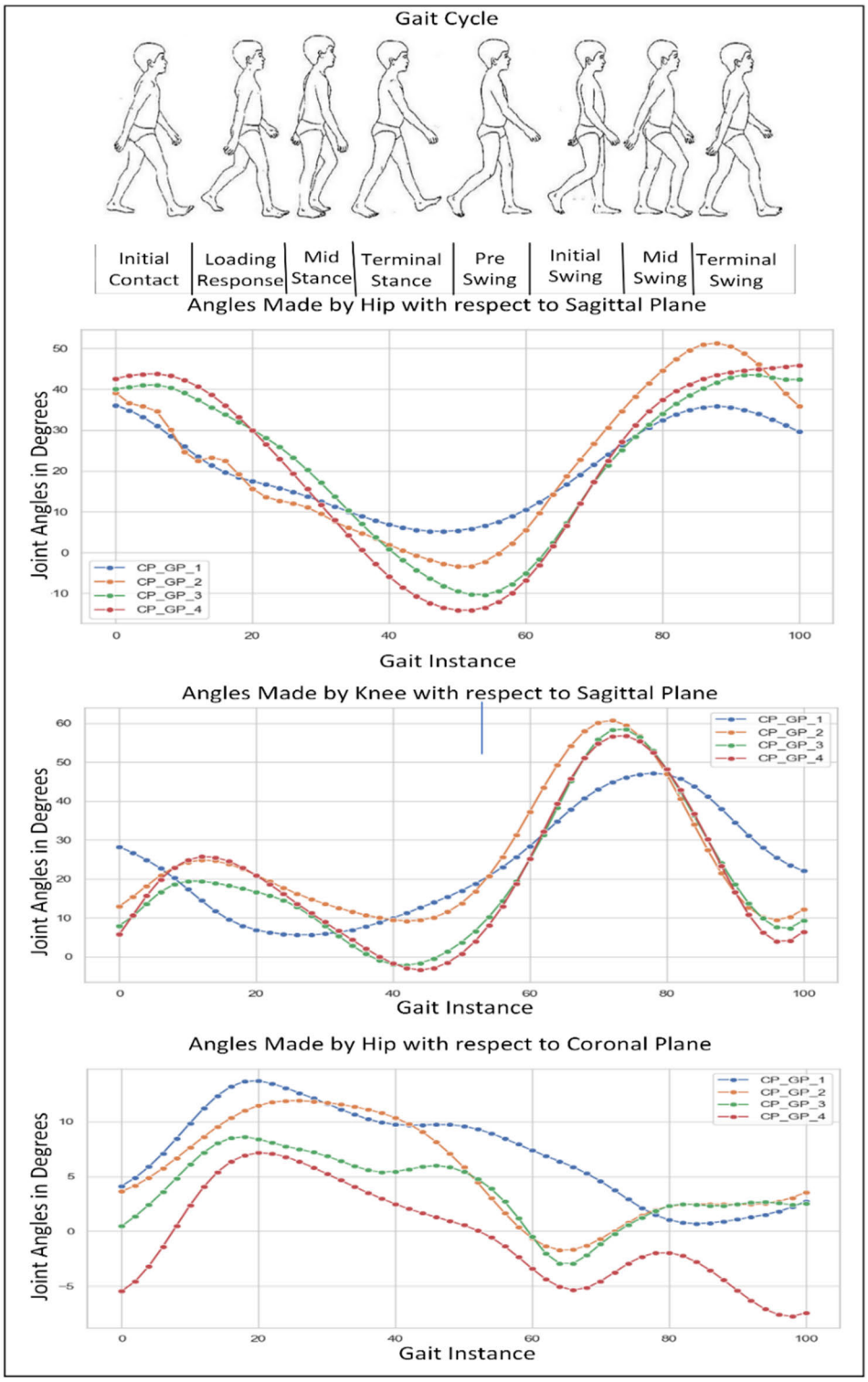

FIGURE 5. Joint angles made with respect to different planes in Cerebral Palsy gait.

using Seaborn's heatmap function. Numerous factors, including the colormap selection, can be customized with this function. Each heatmap image is uniquely identified by its corresponding row index number. The heatmap is saved as an image file into the appropriate folders based on the row index and feature after it has been created. With this all-inclusive method, the raw signal data is converted into visually appealing heatmap images that reveal the temporal evolution of gait

characteristics.

$$H(Xm) = sns.heatmap\{S'mn, viridis, xticklabels, yticklabels, cbar\_kws\} \quad (4)$$

where, '*viridis*' is the colormap used, '*xticklabels*' is time instances during gait cycle, '*yticklabels'* are values of joint angles made, '*cbar_kws*' is the color bar properties dictionary.

According to the method described in this data preprocessing, 1719 samples in the dataset converted to heatmaps. All seven features underwent the same comprehensive conversion from csv data to heatmap images. The data preprocessing is followed by implementing the algorithm on processed data. Coser et al. [38] stated that certain AI algorithms are particularly well-suited for taking on particular tasks.

C. PROPOSED METHODOLOGY

1) GAN IMPLEMENTATION

The proposed research utilized GANs to add synthetic data to the original dataset, increasing its diversity and scalability for further analysis as the gait dataset exhibits a class imbalance. Consequently, GAN was used to enhance the samples in particular classes b, c, and d. GAN required adversarial training of a discriminator network and a generator. Here, artificial images that mimic genuine photos are produced using GANs. By adding GAN generated images to the dataset, this may enhance the performance of models that have been trained on it. The original image's pixel values are normalized from [0, 255] to the range of [0, 1] in the preprocessing step, and they are downsized from 1024 × 1024 pixels to 64 × 64 pixels. We will obtain the created images from the generator after the original images are prepared. A probability score function is assigned by the discriminator which indicates the similarity of generated image to the original image. Discriminator computes the binary cross entropy, and modifies the discriminator's weights in order to minimize the loss. Additionally, we will be able to compute the generator's loss based on the discriminator's output. To optimize the generator's capacity to produce images that the discriminator recognizes as authentic, its weights are modified. Gradient ascent is used to update the generator weights. This process is carried out throughout several epochs. The ConvLSTM algorithm is trained using both the original and generated images. In figure 7, a thorough description of the generator and discriminator models that were employed is presented.

The generator model that was discussed is a sequential model made up of two layers: Conv2DTranspose Layer 1 and Conv2DTranspose Layer 2, as well as a dense layer and a reshape layer. The output of the dense layer is reshaped by the reshape layer into a 3D tensor with dimensions (8, 8, 128). Conv2DTranspose Layer 1 upsamples the tensor by applying the transposed convolution process through 64 filters with ReLU activation function. It expands the dimensions of space. Additionally, 64 filters with the ReLU activation function make up Conv2DTranspose Layer2, which further upsamples the tensor. The output images from this layer have three channels, with 0 to 1 values for each pixel. Conv2D Layer1, Conv2D Layer2, flatten layer, and dense layer make up this discriminator. Conv2D layer 1 processes the input image by applying 64 filters in order to identify features. This layer uses operations, just like the previous Conv2D layer, to find features in a deeper layer.

The output tensor is flattened by the flatten layer, turning it from a 3D tensor to a 1D tensor. The likelihood that the input image is real is represented by a single value between 0 and 1, which is produced by the output dense layer of the discriminator. Here, 64 filters are used by Conv2D layer 1 to scan the input image and detect various features. Feature extraction and learning the hierarchical representation of the input photos are done using Conv2D layer 2. The 3D tensor (128 × 128×3) is transformed into a 1D tensor using the flatten layer. Every slice in the input tensor is taken and arranged into a single row. When switching from convolutional layers, which work with spatial parameters, to dense layers, which require a 1D output, this process is required. The images are resized to 50×148×3 to make it compatible with ConvLSTM and original set of images. Figure 6 displays the GAN model used for synthetic data generation. Reliability of GAN generated images are increased by means of transparent reporting and rigorous validation procedures, which include biological realism and statistical distribution comparisons of the generated samples. This justifies the dataset's appropriateness for driving biomedical research and supporting clinical decision-making.

2) CONVLSTM MODEL

The abnormal gait patterns linked to CP were sequence classified using convolutional long short-term memory networks. In order to comprehend sequential visual input, figure 7 displays the ConvLSTM model architecture which makes use of the unique abilities of LSTM layers to capture long-range correlations. The model combines layers of Long Short-Term Memory (LSTM) and Convolutional Neural Network (CNN) to offer a comprehensive approach to temporal modeling and feature extraction. The ConvLSTM model is designed to extract both spatial and temporal features from sequential image data. Because the model includes convolutional filters and LSTM layers, it can capture both spatial patterns and temporal dependencies. Here, the height, width, and RGB color channels are indicated by the numbers 50, 148, and 3, respectively, for both the original and GAN-generated images. The Conv2D layer 1 applies filters to the input images to extract features. The first Conv2D layer with 32 filters uses a 3 × 3 kernel to identify basic features in the input pictures. Using successively bigger filter sizes, subsequent Conv2D layer 2 (64 and 128) captures more complex and abstract elements. The spatial dimensions of the feature maps are decreased by MaxPooling2D layers selecting the largest value in each local location. Pooling helps to preserve important traits when the spatial resolution is reduced. The TimeDistributed wrapper makes it easier for the LSTM layers to process data

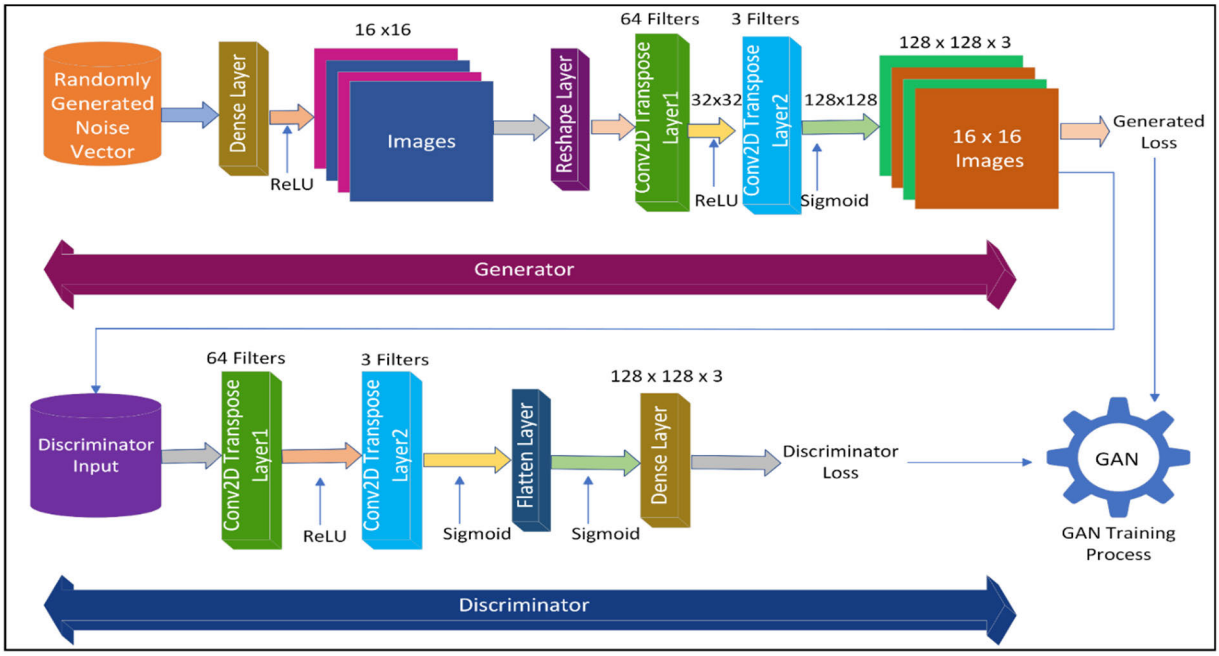

FIGURE 6. GAN model.

sequences. LSTM layers can be used with time-series or video data because they are designed to capture temporal dependencies in sequences. The first TimeDistributed LSTM layer is responsible for processing the series of feature maps that are obtained by the convolutional layers. The TimeDistributed Flatten layer converts the output from the LSTM layer into a flat vector for each time step. It prepares the data for the LSTM layer that comes next. The second LSTM layer is still capturing the temporal dependencies in the sequence.

$$h_{h,t},, c\ h, t = LSTM\left(X_{h,t}, h_{h,t} - 1, c\ h, t - 1\right) \quad (5)$$

$$h_{a,t}, Ca, \mathrm{t} = LSTM\left(X_{a,t}, h_a, t - 1, c_{a,t} - 1\right) \quad (6)$$

$$h_{k,t}, c\ k, \mathrm{t} = LSTM\left(X_{k,\mathrm{t}}, h_{k,\mathrm{t}} - l, c\ k, \mathrm{t} - l\right) \quad (7)$$

The above equations (5), (6) and (7) states that the LSTM layer processes the hip, ankle and knee angle sequence X_h, X_a, X_k at each time step t, will update the hidden state and cell state $h_{h,t}t, ch, t, h_{a,t}, ca, t, h_{k,t}, ck, t$ based on the input $X_{h,t}, X_{a,t}, X_{k,t}$ and previous states $h_k, t - l, c\ h, t - 1, h_a, t - l, c_a, \mathrm{t} - 1, h\ k, \mathrm{t} - 1, c\ k, \mathrm{t} - 1$.

The output from the second LSTM layer is used by the Flatten layer to construct a one-dimensional vector.

$$Flatten\ (X_h) = reshape\ (X_h, (32\ , hip\_time\_steps, -1\ )) \quad (8)$$

$$Flatten\ (X_a) = reshape\ \left(X_{a_,}, (32\ , ankle\_time\_steps, -1\ )\right) \quad (9)$$

$$Flatten\ (X_k) = reshape\ (X_k, (32\ , knee\_time\_steps, -1\ )) \quad (10)$$

The above equations (8), equation (9), equation (10) reshapes the output sequence of hip, ankle and knee data from the LSTM layer. Then we will concatenate the temporal information of flattened sequences.

$$Concatenate(Flatten\ (X_h)\ , Flatten\ (X_a)\ , Flatten\ (X_k)) \quad (11)$$

The above equation (11) shows the concatenation of flattened sequences.

Dense layers are fully connected layers that give the network additional non-linearity. In the first Dense layer, 100 neurons have ReLU activation.

$$Y_{densel} = \sigma\ (W_{densel} \cdot\ Concatenated\_Inputs + bdensel) \quad (12)$$

The above equation (12) shows the application of fully connected layer with ReLU activation to concatenated sequence that is equation (11).

The second Dense layer (output layer) uses softmax activation to create class probabilities for multi-class classification. The Adam optimizer is used in the training setup, with a custom learning rate of 0.001.

$$Y_{output} = softmax\left(W_{output} \cdot Y_{densel} + b_{output}\right) \quad (13)$$

The output layer which is represented by (13) applies softmax activation function to give abnormal gait probabilities. Vital hyperparameters are used by the ConvLSTM model described in this research to influence the model's training and classification procedures. The Adam optimizer is used for optimization, and its learning rate is set to 0.001. During

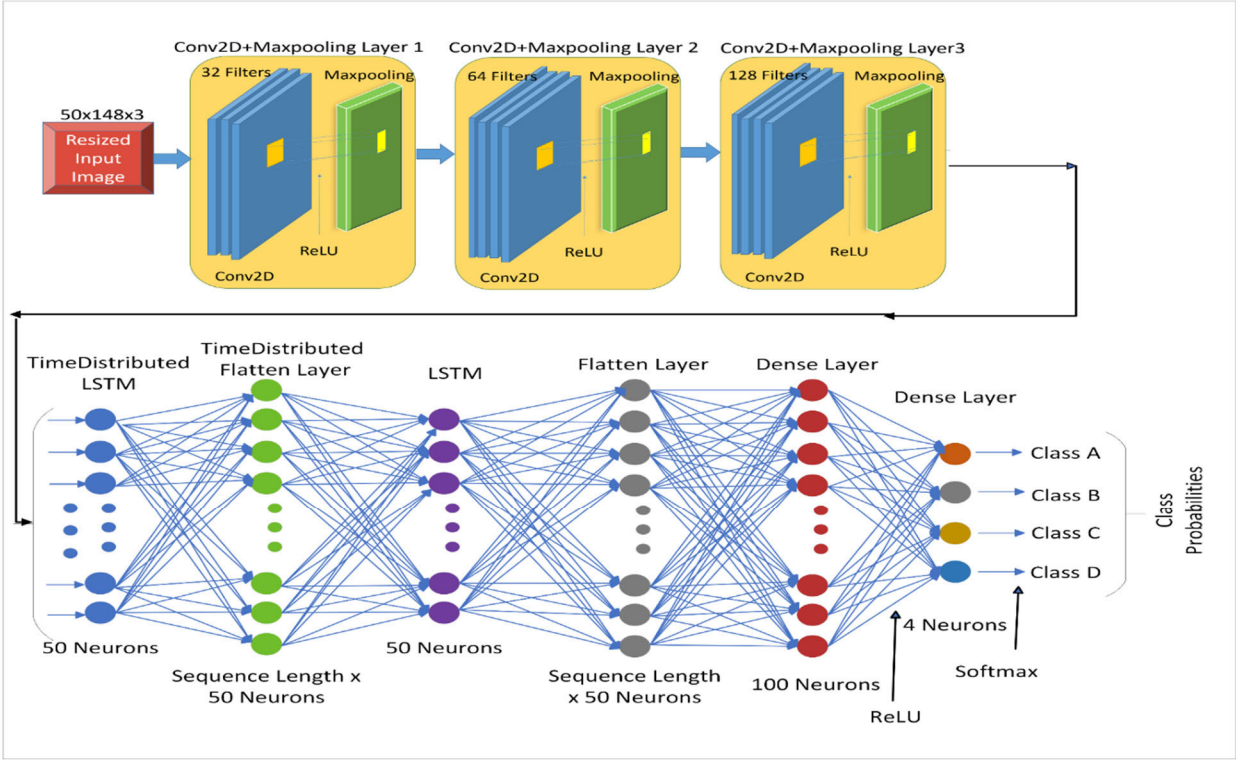

FIGURE 7. ConvLSTM model.

training, this optimizer choice allows for efficient gradient-based updates. The categorical crossentropy loss function, which evaluates the difference between expected and actual class probabilities, is used to assess the model's performance during training. Each iteration of the training process involves processing data batches of size 32 over a period of 50 epochs. Additionally, 20% of the dataset is set aside for validation in order to track the model's capacity for generalization. Image preprocessing is converting pixel values to a range of 0 to 1, which promotes more stable convergence and increases training efficiency. Together, these carefully selected hyper-parameters support the ConvLSTM model's efficiency in image sequence classification task of abnormal gait classification in children with CP. The proposed model achieved an accuracy of 91.8% and loss 0.42. Figure 8 displays the confusion matrix.

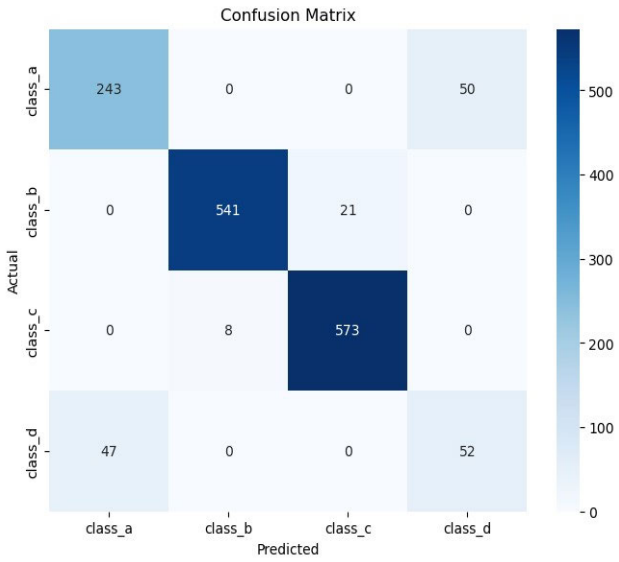

FIGURE 8. Confusion matrix for ConvLSTM.

IV. RESULTS AND ANALYSIS

The total accuracy of roughly 91.8% and loss function 0.41 indicates that the ConvLSTM model is doing a good job of classifying abnormal gait in people with CP, especially when combined with the usage of Generative Adversarial Networks (GANs) to generate extra images. It is impressive how well the model performs with a small dataset and can generalize. The model can capture both temporal and spatial correlations in gait data because of the use of ConvLSTM, which makes it appropriate for applications like abnormal gait classification.

Here the individual class accuracies for class A, B, C and D are 82.9%, 96.3%, 98.6% and 52.5% respectively. A confusion matrix is created based on the model's predictions for classes A, B, C, and D, as depicted in figure 10. The other performance metrics values are also calculated based on the true positives, true negatives, false positives and false negatives from the confusion matrix. The other performance metrics

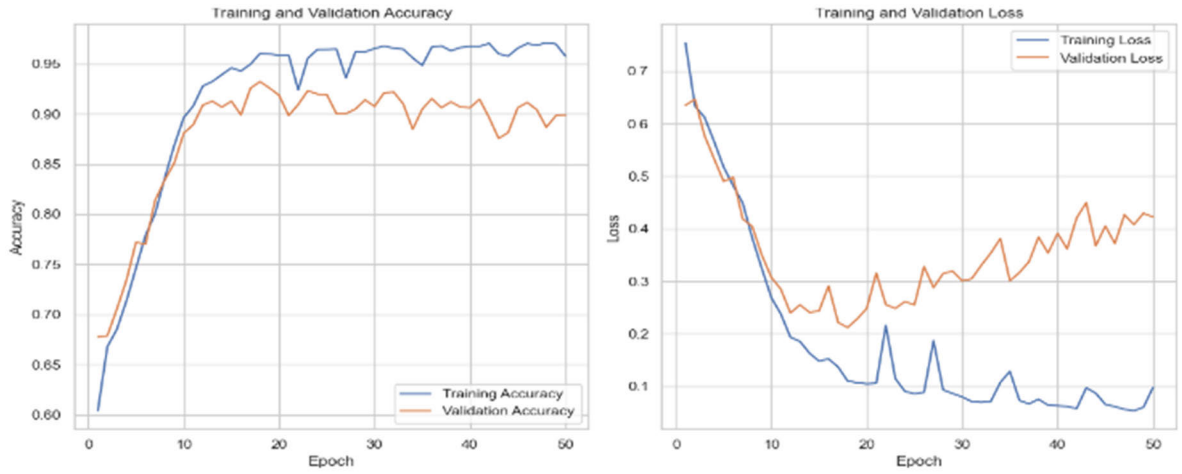

FIGURE 9. ConvLSTM performance graph.

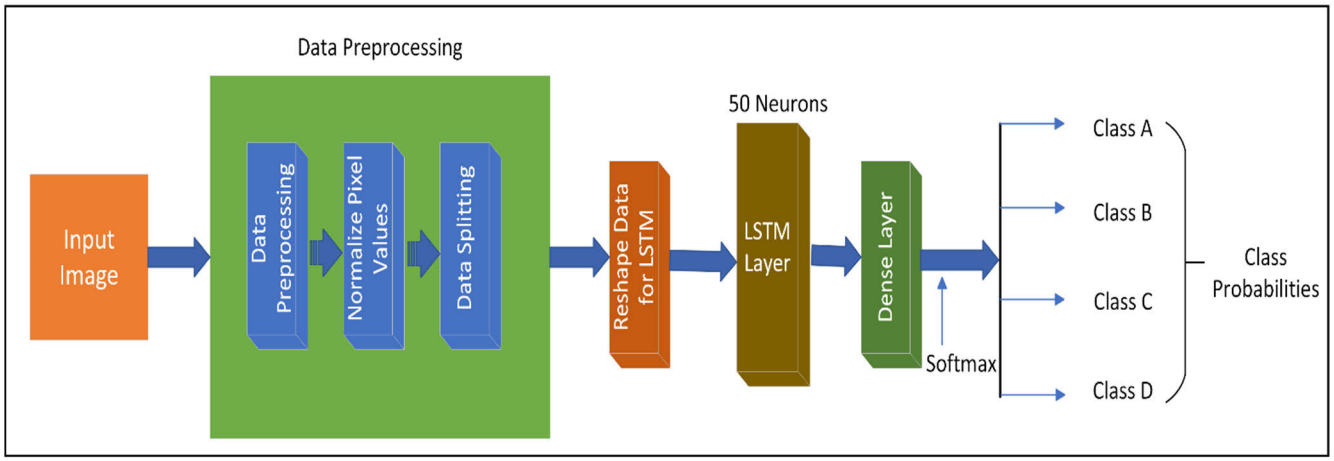

FIGURE 10. Long short term memory model.

values for this model are 82.9%, 100%, 100%, 89.4%, 17% and 0% for Sensitivity, Specificity, Precision, F1 score, False Rejection Rate(FRR), False Positive Rate(FPR) respectively.

A. COMPARISION WITH OTHER MODELS

1) LONG SHORT TERM MEMORY MODEL

Preparation in LSTM model entails transforming the labels lists and data into arrays, is a prerequisite before moving further with this paradigm. Testing and training sets of data were created. To fall between [0, 1], the image's pixel values are changed and the class labels' one-hot encoding was changed. This stage is critical in categorical classification situations where a model has to predict one of the supplied classes. The data is transformed into a three-dimensional array, where the third dimension represents the flattened pixel values of the original images. A sequential model was developed with Keras. Now that the LSTM layer has 50 neurons, it is prepared to take in image sequences as input.

The number of neurons in the LSTM layer represents the dimensionality of the output space. The output of the LSTM is input into a dense layer that has been triggered using softmax to provide the final classification as illustrated in the figure 10.

The model is trained on the training set for 50 epochs with a batch size of 32. The performance of the LSTM model is assessed using test data, and graphs of accuracy and loss function are created over a 50-epoch period. The graph that follows in figure 11 illustrates how the LSTM model performed during training, achieving a validation accuracy of 77.03% and a corresponding loss of 0.47.

2) CONVOLUTIONAL NEURAL NETWORK MODEL

In CNN model, images from different classes, both original and produced by GANs, are loaded and labeled. After being transformed into NumPy arrays, the data is divided into training and testing sets. Pixel values in an image are normalized to fall between [0, 1]. The preprocessed data is now fed into

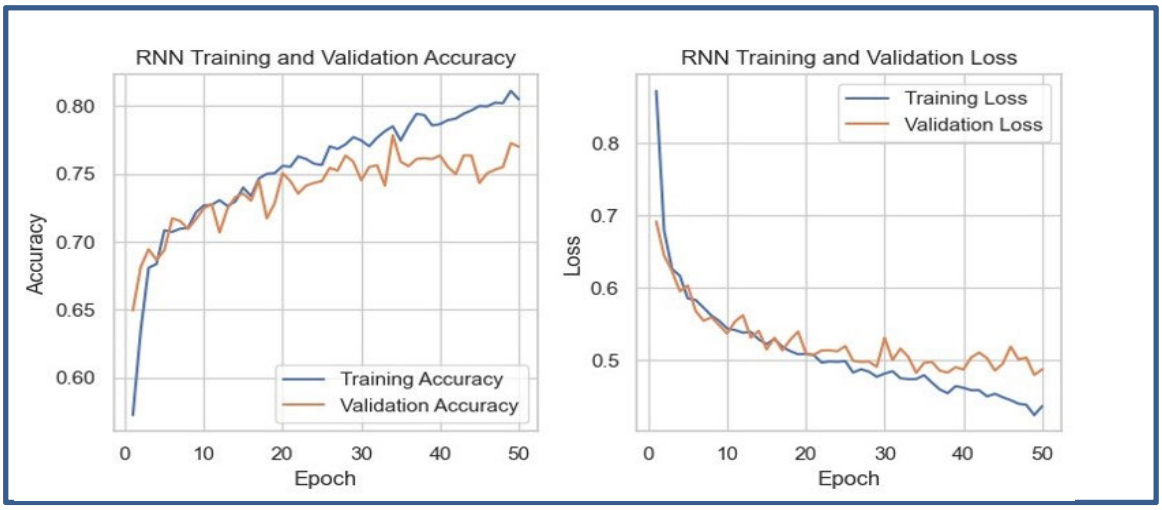

FIGURE 11. The long short term memory performance graph.

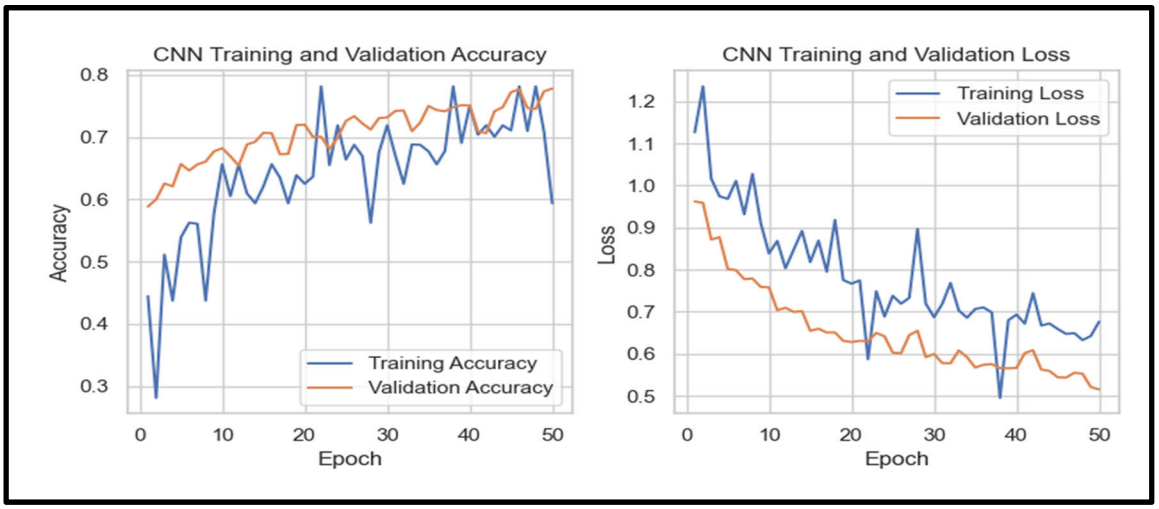

FIGURE 12. Convolutional neural network performance graph.

from the CNN design, which has two convolutional layers and a max-pooling layer for each.

The data for the dense layer is ready because of the flattened layer. The final classification into categories for abnormal gait is done by the dense layer using the softmax activation function. The Adam optimizer is used to compile the model. According to the observations made from CNN performance graph of figure 12, the CNN model did reasonably well during training, achieving a validation accuracy of 79% and a corresponding loss of 0.52.

3) GATED RECURRENT UNIT MODEL

In the initial step of Gated Recurrent Unit (GRU) model, each class, labels and images are loaded. The labels list contains the corresponding labels. The lists of labels and data are transformed into NumPy arrays. There are training and testing sets of the data. The photos' pixel values are adjusted to fall between [0, 1]. We convert categorical labels to one-hot encoding. To satisfy the GRU model's requirements, the input data is rearranged. The temporal dimension is retained even when the images are flattened along their height and breadth dimensions. Keras is used to generate a sequential model. To the model, a 50-unit GRU layer is introduced. The reshaped data is used to specify the input shape.

To classify the data into the designated number of classes, a dense layer with softmax activation is implemented. The Adam optimizer and categorical cross entropy loss function are used to train the GRU model. Iterating over the dataset many times, the training is carried out for 50 epochs. On the validation dataset, the accuracy of the GRU model was 85.6%. The difference between the actual and anticipated class probabilities is 0.45 as depicted in the GRU performance figure 13. Table 2 shows the performance metrics of proposed method compared with all other models CNN, LSTM and

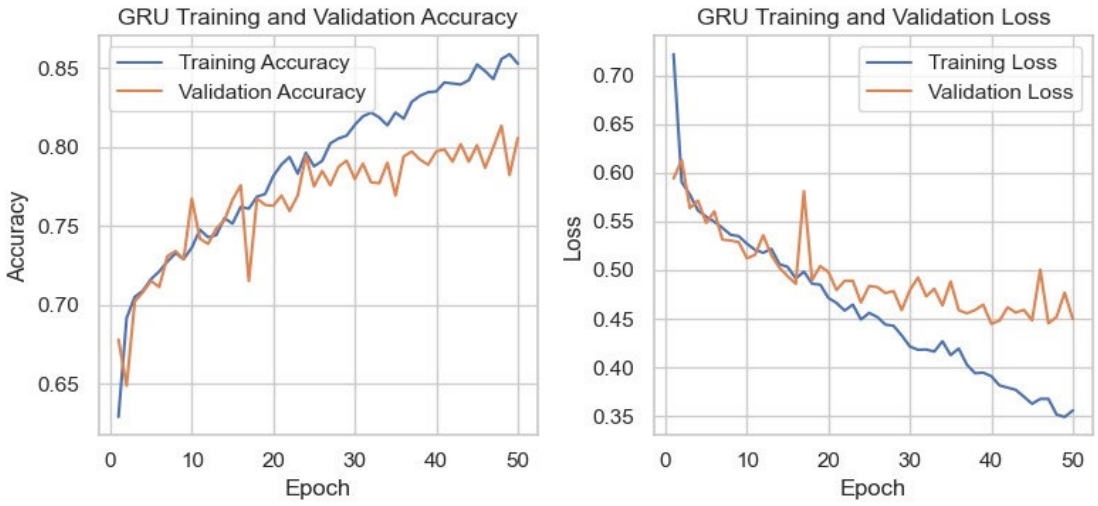

FIGURE 13. Gated recurrent unit performance graph.

TABLE 2. Comparision of performance metrics of convlstm with other models.

Metric/Model	CNN	LSTM	GRU	ConvLSTM(Proposed)
Task	Abnormal gait classification in children with CP	Abnormal gait classification in children with CP	Abnormal gait classification in children with CP	Abnormal gait classification in children with CP
Dataset Used	Gait analysis data of children with Cerebral Palsy [35]	Gait analysis data of children with Cerebral Palsy [35]	Gait analysis data of children with Cerebral Palsy [35]	Gait analysis data of children with Cerebral Palsy [35]
Accuracy	79.82%	76.89%	82.9%	**91.8%**
Loss Function	0.51	0.48	0.45	**0.41**
Sensitivity	75.81%	75.24%	78.64%	**82.9%**
Specificity	100%	100%	100%	100%
F1 Score	78.30%	80.38%	82.28%	**89.4%**
Precision	80.98%	83.17	86.28%	**100%**
FPR	9.33%	8.28%	6.80%	**0%**
FRR	19%	18%	18%	**17%**

GRU where the proposed model achieved impressive metric values.

V. CONCLUSION

The proposed methodology aims to improve the quality of gait analysis in children with CP by integrating state-of-the-art methods in generative modeling, image transformation, and time series analysis seamlessly. This will provide a reliable and interpretive framework for understanding and categorizing gait abnormalities. By combining ConvLSTM, temporal signal data conversion to images, and GAN-based data augmentation, the state-of-the-art in abnormal gait analysis-based early-stage CP identification is being advanced. The ConvLSTM model has demonstrated a remarkable accuracy rate of 91.8%, outperforming other well-established models such as CNN, LSTM, and GRU. This remarkable precision highlights how well our suggested approach captures complex patterns in gait data. In addition, the extremely low loss function of 0.41 indicates how well it minimizes prediction errors.

VI. LIMITATIONS AND FUTURE SCOPE

Notably, the accuracy for Class D abnormal gait category is lower compared with other classes. Numerous reasons could be the cause of this decreased accuracy. The model's capacity for successful generalization have been hampered by the scant data available for Class D. Even when GAN images are used for data augmentation, there may still be a

constraint in producing enough diverse data for a particular class with fewer cases overall. Furthermore, the intrinsic diversity Class D may make it more challenging to identify representative patterns, especially the data that is currently available does not accurately reflect the whole range of anomalies that fall into this category.

Future work should concentrate on enlarging the dataset with more abnormal gait data samples from Class D in order to effectively address this limitation. We can improve the consistency and precision of the suggested ConvLSTM model by adding a wider range of abnormal gaits related to class D. In addition to that, other marker trajectories at trunk and pelvis can be analyzed for the classification of abnormal gait patterns. Angles made by marker trajectories with respect to transverse imaginary plane can also be considered for classification of abnormal gait types in CP.

REFERENCES

[1] Cerebral Palsy Alliance Research Foundation. (2020). *Cerebral Palsy Facts | Cerebral Palsy Alliance Research Foundation*. Accessed: Aug. 5, 2024. [Online]. Available: https://cparf.org/what-is-cerebral-palsy/facts-about-cerebral

[2] (Oct. 12, 2023). *Cerebral Palsy Statistics | Facts and Insights on CP*. Cerebral Palsy Guide. [Online]. Available: https://www.cerebralpalsyguide.com/cerebral-palsy/statistics

[3] A. J. Spittle, C. Morgan, J. E. Olsen, I. Novak, and J. L. Y. Cheong, "Early diagnosis and treatment of cerebral palsy in children with a history of preterm birth," *Clinics Perinatol.*, vol. 45, no. 3, pp. 409–420, Sep. 2018, doi: 10.1016/j.clp.2018.05.011.

[4] C. Sankar and N. Mundkur, "Cerebral palsy-definition, classification, etiology and early diagnosis," *Indian J. Pediatrics*, vol. 72, no. 10, pp. 865–868, Oct. 2005, doi: 10.1007/bf02731117.

[5] C. Bayón, M. Hoorn, A. Barrientos, E. Rocon, J. P. Trost, and E. H. F. Asseldonk, "Perspectives on ankle-foot technology for improving gait performance of children with cerebral palsy in daily-life: Requirements, needs and wishes," *J. Neuroeng. Rehabil.*, vol. 20, no. 1, no. 44, Apr. 2023, doi: 10.1186/s12984-023-01162-3.

[6] Y. Ma, K. Zhang, S. Li, L. Wang, and T. Wang, "Biomechanical analysis of gait patterns in children with intellectual disabilities," *J. Intellectual Disability Res.*, vol. 65, no. 10, pp. 912–921, Aug. 2021, doi: 10.1111/jir.12872.

[7] P. E. Morgan, S. E. Soh, and J. L. McGinley, "Health-related quality of life of ambulant adults with cerebral palsy and its association with falls and mobility decline: A preliminary cross sectional study," *Health Qual. Life Outcomes*, vol. 12, no. 1, p. 132, Aug. 2014, doi: 10.1186/s12955-014-0132-1.

[8] M. Domagalska-Szopa and A. Szopa, "Gait pattern differences among children with bilateral cerebral palsy," *Frontiers Neurol.*, vol. 10, p. 183, Mar. 2019, doi: 10.3389/fneur.2019.00183.

[9] H. Piitulainen, J.-P. Kulmala, H. Mäenpää, and T. Rantalainen, "The gait is less stable in children with cerebral palsy in normal and dual-task gait compared to typically developed peers," *J. Biomech.*, vol. 117, Mar. 2021, Art. no. 110244, doi: 10.1016/j.jbiomech.2021.110244.

[10] M. Asif, M. A. Tayyab, M. H. Shahid, U. Arif, M. I. Tiwana, U. S. Khan, and W. S. Qureshi, "Analysis of human gait cycle with body equilibrium based on leg orientation," *IEEE Access*, vol. 10, pp. 123177–123189, 2022, doi: 10.1109/ACCESS.2022.3222859. https://doi.org/10.1109/access.2022.3222859

[11] L. Carcreff, C. N. Gerber, A. Paraschiv-Ionescu, G. De Coulon, K. Aminian, C. J. Newman, and S. Armand, "Walking speed of children and adolescents with cerebral palsy: Laboratory versus daily life," *Frontiers Bioeng. Biotechnol.*, vol. 8, p. 812, Jul. 2020, doi: 10.3389/fbioe.2020.00812.

[12] R. M. Kanko, E. K. Laende, G. Strutzenberger, M. Brown, W. S. Selbie, V. DePaul, S. H. Scott, and K. J. Deluzio, "Assessment of spatiotemporal gait parameters using a deep learning algorithm-based markerless motion capture system," *J. Biomech.*, vol. 122, Jun. 2021, Art. no. 110414, doi: 10.1016/j.jbiomech.2021.110414.

[13] Z. A. Hussein, I. A. Salem, and M. S. Ali, "Effect of simultaneous proprioceptive-visual feedback on gait of children with spastic diplegic cerebral palsy," *J. Musculoskeletal Neuronal Interact.*, vol. 19, no. 4, pp. 500–506, Dec. 2019.

[14] E. A. Steffensen, F. Magalhães, B. A. Knarr, and D. C. Kingston, "Comparison of markerless and marker-based motion capture of gait kinematics in individuals with cerebral palsy and chronic stroke: A case study series," *Res. Square*, vol. 1, no. 1, pp. 1–12, Feb. 2023.

[15] J. Lorentzen, R. Frisk, M. Willerslev-Olsen, L. Bouyer, S. F. Farmer, and J. B. Nielsen, "Gait training facilitates push-off and improves gait symmetry in children with cerebral palsy," *Hum. Movement Sci.*, vol. 69, Feb. 2020, Art. no. 102565, doi: 10.1016/j.humov.2019.102565.

[16] J. Feng, J. Wick, E. Bompiani, and M. Aiona, "Applications of gait analysis in pediatric orthopaedics," *Current Orthopaedic Pract.*, vol. 27, no. 4, pp. 455–464, Jul. 2016, doi: 10.1097/BCO.0000000000000386.

[17] Y. Ma, K. Mithraratne, N. C. Wilson, X. Wang, Y. Ma, and Y. Zhang, "The validity and reliability of a Kinect v2-based gait analysis system for children with cerebral palsy," *Sensors*, vol. 19, no. 7, p. 1660, Apr. 2019, doi: 10.3390/s19071660.

[18] L. M. Oudenhoven, L. F. van Vulpen, A. J. Dallmeijer, S. de Groot, A. I. Buizer, and M. M. van der Krogt, "Effects of functional power training on gait kinematics in children with cerebral palsy," *Gait Posture*, vol. 73, pp. 168–172, Sep. 2019, doi: 10.1016/j.gaitpost.2019.06.023.

[19] M. Wesseling, H. Kainz, T. Hoekstra, S. Van Rossom, K. Desloovere, F. De Groote, and I. Jonkers, "Botulinum toxin injections minimally affect modelled muscle forces during gait in children with cerebral palsy," *Gait Posture*, vol. 82, pp. 54–60, Oct. 2020, doi: 10.1016/j.gaitpost.2020.08.122.

[20] P. K. Gill, K. M. Steele, J. M. Donelan, and M. H. Schwartz, "Causal modelling demonstrates metabolic power is largely affected by gait kinematics and motor control in children with cerebral palsy," *PLoS ONE*, vol. 18, no. 5, May 2023, Art. no. e0285667, doi: 10.1371/journal.pone.0285667.

[21] N. Dursun, M. Bonikowski, E. Dabrowski, D. Matthews, M. Gormley, A. Tilton, J. Carranza, A.-S. Grandoulier, P. Picaut, and M. R. Delgado, "Efficacy of repeat abobotulinumtoxinA (Dysport) injections in improving gait in children with spastic cerebral palsy," *Develop. Neurorehabil.*, vol. 23, no. 6, pp. 368–374, Nov. 2019, doi: 10.1080/17518423.2019.1687602.

[22] B. L. Shideler, T. C. Bulea, J. Chen, C. J. Stanley, A. J. Gravunder, and D. L. Damiano, "Toward a hybrid exoskeleton for crouch gait in children with cerebral palsy: Neuromuscular electrical stimulation for improved knee extension," *J. Neuroeng. Rehabil.*, vol. 17, no. 1, p. 121, Sep. 2020, doi: 10.1186/s12984-020-00738-7.

[23] A. J. Ries and M. H. Schwartz, "Ground reaction and solid ankle–foot orthoses are equivalent for the correction of crouch gait in children with cerebral palsy," *Develop. Med. Child Neurol.*, vol. 61, no. 2, pp. 219–225, Aug. 2018, doi: 10.1111/dmcn.13999.

[24] J. Snodgrass, J. Snodgrass, S. Yan, H. Lim, I. Hameedduddin, and M. Wu, "Design and implementation of a portable knee actuator for the improvement of crouch gait in children with cerebral palsy," in *Proc. PubMed*, Jul. 2023, pp. 1–4, doi: 10.1109/embc40787.2023.10341076.

[25] D. X. Liu, W. Du, X. Wu, C. Wang, and Y. Qiao, "Deep rehabilitation gait learning for modeling knee joints of lower-limb exoskeleton," in *Proc. IEEE Int. Conf. Robot. Biomimetics (ROBIO)*, Dec. 2016, pp. 1058–1063, doi: 10.1109/robio.2016.7866465.

[26] P. Khera and N. Kumar, "Role of machine learning in gait analysis: A review," *J. Med. Eng. Technol.*, vol. 44, no. 8, pp. 441–467, Nov. 2020.

[27] R. Kolaghassi, G. Marcelli, and K. Sirlantzis, "Deep learning models for stable gait prediction applied to exoskeleton reference trajectories for children with cerebral palsy," *IEEE Access*, vol. 11, pp. 31962–31976, 2023, doi: 10.1109/ACCESS.2023.3252916. https://doi.org/10.1109/access.2023.3252916

[28] M. E. Ozates, D. Karabulut, F. Salami, S. I. Wolf, and Y. Z. Arslan, "Machine learning-based prediction of joint moments based on kinematics in patients with cerebral palsy," *J. Biomech.*, vol. 155, Jun. 2023, Art. no. 111668, doi: 10.1016/j.jbiomech.2023.111668.

[29] R. Gautam and M. Sharma, "Prevalence and diagnosis of neurological disorders using different deep learning techniques: A meta-analysis," *J. Med. Syst.*, vol. 44, no. 2, p. 49, Jan. 2020, doi: 10.1007/s10916-019-1519-7.

[30] M. Lempereur, F. Rousseau, O. Rémy-Néris, C. Pons, L. Houx, G. Quellec, and S. Brochard, "A new deep learning-based method for the detection of gait events in children with gait disorders: Proof-of-concept and concurrent validity," *J. Biomech.*, vol. 98, Jan. 2020, Art. no. 109490, doi: 10.1016/j.jbiomech.2019.109490.
[31] A. M. Al-Sowi, N. AlMasri, B. Hammo, and F. A.-Z. Al-Qwaqzeh, "Cerebral palsy classification based on multi-feature analysis using machine learning," *Informat. Med. Unlocked*, vol. 37, Jan. 2023, Art. no. 101197, doi: 10.1016/j.imu.2023.101197.
[32] Y. Zhang and Y. Ma, "Application of supervised machine learning algorithms in the classification of sagittal gait patterns of cerebral palsy children with spastic diplegia," *Comput. Biol. Med.*, vol. 106, pp. 33–39, Mar. 2019, doi: 10.1016/j.compbiomed.2019.01.009.
[33] P. Patil, K. S. Kumar, N. Gaud, and V. B. Semwal, "Clinical human gait classification: Extreme learning machine approach," in *Proc. 1st Int. Conf. Adv. Sci., Eng. Robot. Technol. (ICASERT)*, May 2019, pp. 1–6, doi: 10.1109/ICASERT.2019.8934463.
[34] Ł. Kidziński, S. Delp, and M. Schwartz, "Automatic real-time gait event detection in children using deep neural networks," *PLoS ONE*, vol. 14, no. 1, Jan. 2019, Art. no. e0211466, doi: 10.1371/journal.pone.0211466.
[35] S. Potluri, S. Ravuri, C. Diedrich, and L. Schega, "Deep learning based gait abnormality detection using wearable sensor system," in *Proc. PubMed*, Jul. 2019, pp. 3613–3619, doi: 10.1109/embc.2019.8856454.
[36] K. D. McCay, E. S. L. Ho, H. P. H. Shum, G. Fehringer, C. Marcroft, and N. D. Embleton, "Abnormal infant movements classification with deep learning on pose-based features," *IEEE Access*, vol. 8, pp. 51582–51592, 2020, doi: 10.1109/ACCESS.2020.2980269.
[37] Laet, "3D gait analysis data of children with CP used for gait classification," Tinne De Laet, Angela Nieuwenhuys, Eirini Papageorgiou, Kaat Desloovere KU Leuven, Belgium, Tech. Rep., 2017.
[38] O. Coser, C. Tamantini, P. Soda, and L. Zollo, "AI-based methodologies for exoskeleton-assisted rehabilitation of the lower limb: A review," *Frontiers Robot. AI*, vol. 11, Feb. 2024, Art. no. 1341580.

YELLE KAVYA received the bachelor's degree in electronics and communication engineering and the master's degree from the Gokaraju Rangaraju Institute of Engineering and Technology, Hyderabad, Telangana, India, in 2018. She is currently a full-time Research Scholar with the School of Electronics Engineering, Vellore Institute of Technology, Chennai, India. Her research interests include artificial intelligence, deep learning and machine learning for medical diagnosis, human gait, data augmentation techniques, and quantum machine learning.

S. SOFANA REKA is currently an Associate Professor with the School of Electronics Engineering, Vellore Institute of Technology, Chennai. She has published various international journals with high impact factor in her credit. Her research interests include smart grids, embedded systems, machine learning, the Internet of Things, and cyber-physical systems. She is also a reviewer of many SCI journals.